sustainability

MDPI

Article

Valorization of Coffee Pulp: Spray-Dried Hemp Oil Microcapsules Stabilized with Coffee Pectin and Maltodextrin

Ozan Kahraman *, Greg E. Petersen and Christine Fields

Applied Food Sciences Inc., 675-B Town Creek Road, Kerrville, TX 78028, USA; gpetersen@appliedfoods.com (G.E.P.); cfields@appliedfoods.com (C.F.)
* Correspondence: ozan@appliedfoods.com

Abstract

The global challenge of food waste presents an opportunity to explore the untapped potential of agricultural by-products. Coffee pulp, a major by-product of the coffee industry, is a promising source of functional polysaccharides such as coffee pectin, which can be valorized for sustainable applications in food systems. This study investigates the microencapsulation of hemp seed oil—rich in essential fatty acids and bioactive lipids—using coffee pectin and maltodextrin as wall materials via spray drying. Emulsions with varying oil-to-wall ratios were formulated and characterized for viscosity, particle size, and zeta potential. The resultant microcapsules were analyzed for physicochemical properties, encapsulation efficiency, oxidative stability (peroxide value), and *in vitro* release in simulated gastrointestinal fluids. Encapsulation efficiencies ranged from 63.27% to 70.77%, with lower oil content formulations exhibiting higher efficiency. The peroxide values indicated enhanced oxidative stability, with the lowest value (10.69 meq O_2/kg oil) observed in the most efficient encapsulation formulation. Microcapsule morphology analysis confirmed the formation of spherical particles with varying degrees of surface roughness. Release studies demonstrated controlled oil delivery, with higher retention in gastric conditions and progressive release in intestinal fluids. These findings demonstrate the potential of upcycled coffee pulp-derived pectin as a functional, sustainable encapsulant, aligning with circular economy principles and supporting the development of stable bioactive delivery systems for nutraceutical and food applications.

Keywords: coffee pectin; encapsulation; sustainability; by-products; hemp oil

Academic Editor: Marko Vinceković

Received: 5 August 2025
Revised: 26 August 2025
Accepted: 5 September 2025
Published: 10 September 2025

Citation: Kahraman, O.; Petersen, G.E.; Fields, C. Valorization of Coffee Pulp: Spray-Dried Hemp Oil Microcapsules Stabilized with Coffee Pectin and Maltodextrin. *Sustainability* **2025**, *17*, 8152. https://doi.org/10.3390/su17188152

1. Introduction

Hemp seed oil, extracted from *Cannabis sativa* seeds, is widely recognized for its high content of essential fatty acids, antioxidants, and bioactive compounds, making it a valuable ingredient in food, pharmaceutical, and cosmetic formulations. However, its susceptibility to oxidation and environmental degradation significantly limits its stability, shelf life, and broader applicability. To use it in practical formats—such as dry beverage premixes and ready-to-drink extensions (for fortification without rancid notes), bakery dry blends, gummies/soft chews, capsules or sachets for nutraceuticals, and topical creams and serums—formulators require powders that dose cleanly, reconstitute reliably, ship easily, and protect the lipids while delivering them to the desired site (e.g., the gut) during consumption [1–3]. To overcome these limitations, encapsulation technologies have been extensively explored to protect sensitive lipids, improve bioavailability, and enhance functional performance. Among these technologies, spray drying has emerged as a widely used

method due to its cost-effectiveness, scalability, and compatibility with thermally sensitive ingredients. The process involves atomizing emulsified feed solutions into a hot drying chamber, rapidly converting them into dry microcapsules. However, several factors can influence the efficiency and quality of spray-dried products, including shear stress during atomization, interfacial interactions, and thermal degradation during dehydration [4–6]. As a result, careful selection of wall materials is critical to preserving the integrity of encapsulated compounds. Polysaccharide-based carriers, particularly maltodextrin (MD), are commonly used due to their excellent film-forming capacity, low viscosity at high solids, and oxidative protection [7,8]. In this study, spray-drying performance was constrained by a solid feed window that balanced pumpability and yield, a wall matrix at glass transition temperature (Tg) above the dryer outlet to avoid stickiness, and stable droplet formation governed by viscosity and interfacial tension; accordingly, coffee pectin (CP) was included to enhance interfacial stabilization/charge during atomization, while MD was chosen to raise solids and Tg for robust film formation.

In recent years, attention has turned to novel, sustainable encapsulants derived from food industry by-products. CP, extracted from coffee pulp—a major agro-industrial waste—has shown promising functional properties, including biocompatibility, emulsifying ability, and biodegradability. It is an anionic polysaccharide whose galacturonic acid groups are largely deprotonated at this study's working pH, yielding a negative zeta potential and electrostatic stabilization; its degree of esterification, together with its residual protein/acetyl groups, modulates its interfacial adsorption and emulsification performance [9,10]. Its application as an encapsulating agent not only enhances product functionality but also contributes to waste valorization and circular economy initiatives. The combination of CP and MD as dual wall materials offers synergistic advantages for oil encapsulation. CP's film-forming properties support stable microcapsule formation, while MD's high glass transition temperature contributes to oxidative and moisture protection during storage. Prior studies show that pairing MD with gum arabic or whey proteins gives stable emulsions and good microencapsulation yields because the protein/gum arabic provides interfacial activity while MD raises solids and Tg to reduce stickiness [11,12]. In contrast, the MD + CP combination is less explored for hemp seed oil, so data linking emulsion properties to powder performance are limited. Addressing this gap matters because CP is an upcycled, plant-based wall that can reduce reliance on animal proteins and scarce GA, improving sustainability and supply resilience while maintaining performance.

This study investigates the physicochemical properties, oxidative stability, and controlled release behavior of spray-dried hemp oil microcapsules formulated with coffee pectin and maltodextrin. It hypothesized that relative to higher oil loadings, lower oil loadings with CP + MD walls will yield higher encapsulation efficiency and better initial oxidative status (lower peroxide value). Key parameters evaluated include encapsulation efficiency, peroxide value, morphology, wettability, and solubility. *In vitro* release kinetics were also assessed under simulated gastrointestinal conditions to evaluate their potential for targeted delivery. The use of coffee pectin, derived from an underutilized agricultural by-product, is further explored as a model of sustainable material innovation. This approach exemplifies a value-added strategy for converting food waste into functional materials with promising applications in nutraceuticals and functional foods.

2. Materials and Methods

2.1. Materials

Hemp seed oil was provided by Victory Hemp Foods (Carrollton, KY, USA). MD with a maximum dextrose equivalent (DE) value of 20 (on a dry basis) purchased from Spectrum Chemical Mfg. Corp. (New Brunswick, NJ, USA). CP (galacturonic acid content: 77.62%,

methoxy group content: 4.68%, esterification degree: 28.8%) was provided by Vidya Herbs Pvt. Ltd. (Bangalore, India). The core material was hemp seed oil, while the encapsulating wall materials were CP and MD. All other chemicals used were of analytical grade and purchased from Fisher Scientific International Inc. (Pittsburgh, PA, USA).

2.2. Preparation of Hemp Seed Oil Emulsions

Four different emulsions were created according to the method described by Karrar et al. [8] with some modifications. All formulations maintained a constant total solids concentration of 20% (*w*/*w*) to keep atomization and drying conditions comparable across runs and incorporated coffee pectin at a fixed concentration of 4% as the primary emulsifying agent. Maltodextrin was included as a supporting wall material at varying concentrations between 10% and 13%, while hemp seed oil was added as the core component at concentrations ranging from 3% to 6%, as detailed in Table 1. Levels were selected after a brief screening to ensure stable pre-drying emulsions (no visible creaming/phase separation for ~30 min) and pumpable viscosity at 25 °C. Solutions were prepared by dissolving the required amount of coffee pectin and maltodextrin in deionized (DI) water by a magnetic stirrer overnight until the wall materials completely dissolved. Then, the hemp seed oil was slowly added into the mixtures using a homogenizer (Model 850, Thermo Fisher Scientific, Waltham, MA, USA) fitted with a 20 mm diameter probe (Cat. No. 15-340-181) at 10,000 rpm for 5 min in an ice bath, with the temperature maintained below 25 ± 1 °C; homogenization was paused if the temperature approached the upper limit. The experiments were conducted according to Table 1 with three replicates. The pH range of the solutions across the formulas was between 5.50 ± 0.2 and 5.63 ± 0.1.

Table 1. Formulations of emulsion samples before and after spray drying.

Formula	In Emulsions				
	Oil (%)	**Coffee Pectin (%)**	**Maltodextrin (%)**	**Total Solids (%)**	**Core: Wall Ratio**
1	3	4	13	20	3:17
2	4	4	12	20	1:4
3	5	4	11	20	1:3
4	6	4	10	20	3:7
Formula	**In Encapsulated Powder**				
	Oil (%)	**Coffee Pectin (%)**	**Maltodextrin (%)**	**Total Solids (%)**	
1	15	20	65	100	
2	20	20	60	100	
3	25	20	55	100	
4	30	20	50	100	

2.3. Analysis of Emulsion Properties

2.3.1. Particle Size, Electrical Conductivity, and Zeta Potential

The emulsions' particle size (μm) and zeta potential (mV) were determined using dynamic light scattering (DLS) at 25 °C using deionized water as a dispersant. Emulsions were gently inverted and diluted to reach 10–15% obscuration. These measurements were performed with a Litesizer 500 instrument by Anton Paar in Graz, ST, Austria. The instrument utilized a 40 mW semiconductor laser with a wavelength of 658 nm, employing detection angles of back (175°), side (90°), and forward (15°). The dynamic light scattering (DLS) technique quantifies the ongoing movement of particles suspended in a solution,

commonly referred to as Brownian motion [13]. The hydrodynamic diameter was determined using a 2 mL disposable cuvette at a temperature of 25 °C. For zeta potential analysis, the Kalliope 2.2 software was employed at 25 ± 0.1 °C, with an equilibration time of 1 min. Each sample (1 mL) was placed in an omega cuvette without air bubbles. Three replicates were conducted for each sample, involving 100 scans per individual measurement.

Electrical conductivity was measured with a benchtop conductivity meter (Orion Star A211, Thermo Fisher Scientific Inc., Waltham, MA, USA) at 25 °C. Results are reported in mS/cm as the mean of three replicates.

2.3.2. Color and Optical Light Microscopy Images

Based on the CIE L*, a*, and b* color values, a Vista colorimeter (HunterLab, Reston, VA, USA) was used to measure changes in the color of emulsions. The brightness/darkness index was denoted by L* (0 to 100/black to white), a* represents redness/greenness with '+' and '−' values, respectively, and b* signifies yellowness/blueness with '+' and '−' values, respectively. Three measurements (L*, a*, and b* values) were taken for each sample at room temperature. The sample was placed in a 10 mm optical path disposable cuvette with a volume of 2 mL; the baseline was set with deionized water. The instrument was standardized before each session against the manufacturer-certified white tile. The reported values represent the mean of the measurements.

The EVOS XL core imaging system (Thermo Fisher Scientific, Waltham, MA, USA) was used to obtain optical microscope images. Each emulsion droplet was carefully positioned on a microscope slide and examined using a transmitted light system at a 40× magnification.

2.3.3. Viscosity

The emulsions' viscosity was determined with a DV3T AMETEK Brookfield rotational rheometer (Middleboro, MA, USA) at a set temperature of 25.0 ± 0.1 °C and controlled with a solvent trap equipped with an LV3 spindle rotating at a speed of 50 rpm. Samples were loaded and allowed to equilibrate for 5 min before measurements to minimize thixotropic effects before measurement. The measurements were conducted three times. The expected experimental uncertainty for apparent viscosity is based on the standard deviation of triplicates combined with the manufacturer's accuracy; the overall expanded uncertainty (k = 2) is approximately ±3% of reading under our conditions.

2.4. Spray-Drying Process for Microencapsulation

The samples were spray dried with a spray dryer (Mini Spray Dryer B-290, Buchi, Flawil, Switzerland) equipped with a 0.7 mm two-fluid nozzle, operated with a compressed air flow of 40 L/min at a pressure of 3 to 5 bar. A glass cylinder (dryer chamber) has the following dimensions: 450 mm in height and 140 mm in diameter. The dryer had an evaporation rate of 1 L/h and a chamber with a diameter of 70 cm. Prepared emulsions were fed into the drying chamber using a peristatic pumping rate of 3 mL/min at an inlet temperature of 160 ± 5 °C, an outlet temperature of 90 ± 5 °C, and an aspirator rate of 100%. To preserve homogeneity and prevent oil droplet coalescence, the emulsions were gently agitated with a magnetic stirrer as they were fed into the spray dryer. The spray-dried powders were collected from the bottom of the cyclone. All drying operations were carried out in triplicate.

2.5. Analysis of Microencapsulated Powders

2.5.1. Moisture, Water Activity, and Particle Size Distribution

The moisture content of powders was evaluated as a percentage on a wet basis at 105 °C using an MA 160 infrared moisture analyzer (Sartorius, Göttingen, Germany). An AquaLab 4TE dew-point water activity analyzer (METER Group, Pullman, WA, USA) was

used to measure the water activity at 25 °C. The water activity analyzer was calibrated using a 0.76 a_w NaCl solution [14].

Encapsulated powders were individually fed into the particle size analyzer (dry dispersion) (Model PSA 1190, Anton Paar, Graz, Austria). Each sample was utilized with dispersion parameters of 57% vibrator duty cycle, 37 Hz vibrator frequency, and 800 mBar of air pressure. Samples were fed via a vibratory feeder into the dry module; dispersion air pressure was set to 800 mBar (deagglomeration) and kept constant for all runs. The quantification of the particle size distribution was obtained by the Fraunhofer reconstruction method. The data was given as D10, D50, and D90, representing the mean volume diameters of the particles at 10, 50, and 90% cumulative volume, respectively.

2.5.2. Encapsulation Efficiency

Encapsulation efficiency was assessed following the procedure outlined by Tonon et al. [15] with slight modifications. To measure surface oil, 20 mL of hexane was added to 1 g of powder and vortexed for 1 min at room temperature. The resulting solvent mixture underwent filtration using Whatman No. 1 filter paper (MilliporeSigma, Burlington, MA, USA). The powder collected on the filter was washed three times with 10 mL of hexane. The filtrate solution, containing the extracted oil, was then transferred to a preweighed 50 mL conical tube and allowed to evaporate, followed by drying at 90 °C until a constant weight was achieved. Surface oil content was determined by calculating the difference in weight between the initial clean flask and the one containing the extracted oil residue. Total oil was considered equivalent to the initial oil, as hemp oil is non-volatile. The following equation was used to determine encapsulation efficiency:

$$\text{Encapsulation efficiency}(\%) = \frac{\text{Total oil} - \text{Surface oil}}{\text{Total oil}} \times 100 \quad (1)$$

2.5.3. Wettability and Solubility

In the wettability assessment method, the wettability of a powder is defined as the time required for 1 g of the powder to completely disappear from the surface of 100 mL of water at 20 °C. The procedure involves sprinkling the powder evenly over the water, starting a timer upon contact, and stopping it when the entire 1 g of powder vanishes. The recorded disappearance time serves as a quantitative measure of wettability [16].

The powders' solubility was determined using a slightly modified version of the methodology described by Karrar et al. [8]. One gram of powder was mixed with 100 mL of distilled water and stirred for 5 min at room temperature using a magnetic stirrer. Following that, the solution was centrifuged at 3000× *g* at 20 °C for 5 min (Sorvall Legend XTR centrifuge, Thermo Scientific, Osterode am Harz, Germany) with Fiberlite F15-8 fixed angle rotor with 104 mm radius; no filtration was performed prior to centrifugation. An aliquot of 25 mL of the supernatant was placed in a preweighed dish and dried at 105 °C. The powders' solubility was calculated using the given equation.

$$\text{Solubility}(\%) = \frac{W_2 \times 4}{W_1} \times 100 \quad (2)$$

where W_2 is the weight of the solids recovered from a 25 mL supernatant; x4 accounts for the total 100 mL dispersion volume, and W_1 is the weight of the powder in the solution.

2.5.4. Release Characteristics

The *in vitro* release characteristics of microencapsulated hemp oil were examined utilizing a simulated gastrointestinal model following a modified version of the procedure described by Karaca et al. [17].

For the preparation of simulated gastric fluid (SGF), 1.0 g of NaCl and 3.5 mL of 11.6 M HCl were dissolved in 400 mL of water. Following the addition of 0.56 g of pepsin (activity: 10,800 FCC U/mg) to the solution, the pH was adjusted to 1.2 using 0.1 M HCl, and the total volume was then adjusted to 500 mL with water. Simulated intestinal fluid (SIF) was created by dissolving 3.4 g of K_2HPO_4 in 400 mL of water. Following the addition of 38.5 mL of 0.2 M NaOH and 5 g of pancreatin (amylase: 1.3 units/mg), the solution was allowed to be stirred overnight at a temperature of 4 °C. The pH was precisely adjusted to 6.8 by adding either 1 M NaOH or 1 M HCl, and the total volume was then adjusted to 500 mL by adding water.

A 4 g sample of microencapsulated hemp oil was mixed with 50 mL of simulated gastric fluid (SGF) and agitated for 2 h at 37 °C and 100 rpm. The pH was adjusted to 6.8 by adding 1 M NaOH. Then, 50 mL of SIF was added to the sample, which was then agitated for an additional 3 h at a temperature of 37 °C and 100 rpm. The amount of hemp oil released from the microcapsules was determined after exposure to simulated gastric fluid (SGF) and simulated intestinal fluid (SIF). After three separate extractions with 15 mL of hexane, the amount of released oil was measured gravimetrically.

2.5.5. Peroxide Values

The samples were sealed immediately after drying and stored at 4 ± 0.5 °C in the dark. The peroxide value of the encapsulated sample was measured using the AOCS method [18]. To conduct the analysis, 1 g of extracted hemp oil was placed in a 125 mL flask. Subsequently, 6 mL of a 3:2 solution of acetic acid and chloroform was added to the sample and the container was agitated to accelerate the dissolving of the oil. Following this, 0.1 mL of saturated potassium iodide was added to the solution, and the flask was intermittently shaken for 1 min. Afterward, 10 mL of distilled water and 0.1 mL of starch solution were added to the solution. Finally, the solution underwent gradual titration with 0.001 N sodium thiosulfate under continuous agitation until the gray color of the solution nearly disappeared.

The following equation was used to calculate the peroxide value (milliequivalents peroxide/1000 g sample):

$$\mathrm{PV} = \frac{(\mathrm{S} - \mathrm{B}) \times \mathrm{N} \times 1000}{\mathrm{W}} \tag{3}$$

where S is the volume of $Na_2S_2O_3$ added to the sample (mL), B is the volume of $Na_2S_2O_3$ of the blank (mL), N is the normality of the $Na_2S_2O_3$ solution, and W is the sample weight (g).

2.5.6. Bulk Density and Tapped Density

The bulk density and tapped density of the sample powders were measured following the method described by Karrar et al. [8]. The bulk density was determined by weighing a 2 g powder sample using an analytical balance (XS104, Mettler Toledo, Columbus, OH, USA) and then placing it in a 10 mL graduated measuring glass cylinder. The bulk density was calculated using the following equation:

$$\text{Bulk density}\left(\frac{\mathrm{g}}{\mathrm{cm}^3}\right) = \frac{\text{Sample weight (g)}}{\text{Sample volume (cm}^3\text{)}} \tag{4}$$

To determine the tapped density of the samples, 2 g of powder was placed in a 10 mL graduated measuring glass cylinder and carefully tapped 100 times. Following that, TD was determined using the following equation:

$$\text{Tapped density}\left(\frac{\mathrm{g}}{\mathrm{cm}^3}\right) = \frac{\text{Sample weight (g)}}{\text{Tapped sample volume (cm}^3\text{)}} \tag{5}$$

2.5.7. Particle Morphology

The morphology of the spray-dried samples was observed with a scanning electron microscope (SEM) (S 3400N, Hitachi Corp., Tokyo, Japan) in high-vacuum mode. The powder samples were attached to a double-sided adhesive tape mounted on SEM stubs, coated with 3–5 mA gold/palladium under vacuum. Finally, the coated samples were scanned with an accelerating beam voltage of 3 kV with magnifications of 5000×.

2.6. Statistical Analysis

All experiments were conducted in triplicate. The results were expressed as mean value ± standard deviation (S.D.). RStudio 4.5.1 software was used to conduct the statistical analysis of the collected data. Differences between the treatments were assessed by running a one-way ANOVA, followed by conducting Tukey's HSD (SciPy v1.16.1) test. Significant differences among the samples were detected at $p < 0.05$.

3. Results and Discussion

3.1. Physicochemical Properties of Emulsions

3.1.1. Viscosity, Electrical Conductivity, Zeta Potential, and Particle Size

Emulsion viscosity influences encapsulation efficiency by reducing the oscillation and movement of oil droplets during spray drying, which enhances oil retention by minimizing volatile compound loss. Excessive viscosity, however, can reduce oil retention due to slower droplet formation and prolonged exposure during atomization [19,20]. Battista et al. [21] recommend keeping feed viscosity below 300 cP for optimal spray drying atomization. In the formulations (Table 2), viscosity ranged from 12.50 ± 0.2 cP (Formula 1) to 14.89 ± 0.01 cP (Formula 4), increasing with higher oil content (3% to 6%) due to increased internal phase volume, leading to greater flow resistance. CP and MD were used as stabilizers, where coffee pectin (4%) increased viscosity by enhancing emulsion stability, and varying MD levels (10% to 13%) influenced viscosity. Higher MD (13%) in Formula 1 resulted in lower viscosity compared to formulations with a higher oil content. The electrical conductivity of the emulsions increased significantly from 5.77 ± 0.04 mS/cm in Formula 1 to 6.51 ± 0.04 mS/cm in Formula 4 ($p < 0.05$). This increase can be attributed to the higher oil concentration and the resultant change in the distribution of ions within the emulsion. MD concentrations varied inversely with the oil percentage, potentially influencing ion dispersion within the aqueous phase. Higher oil concentrations reduce the effective volume of the aqueous phase, which could lead to increased ion density and electrical conductivity. Because bulk conductivity is governed by the ionic content of the continuous aqueous phase, these differences are more plausibly due to variations in ionic strength and pH arising from CP dissolution (exchangeable $Na^+/K^+/Ca^{2+}$) [22]. All formulations exhibited negative zeta potential values, ranging from −6.00 ± 0.07 mV to −7.17 ± 0.21 mV, indicating that the droplets carried a net negative surface charge. The slightly negative zeta potential of the redispersed microcapsules reflects the wall composition: CP carries deprotonated carboxylate groups at the measurement pH, while MD is non-ionic and dilutes the surface charge. Ions in the dispersant compress the electrical double layer, further reducing [22–25]. The zeta potential did not show a large variation among formulations, but Formula 4, with the highest oil content, had a significantly higher negative zeta potential ($p < 0.05$). Across Formula 1 to Formula 4, zeta potential values (mean ± SD) were −7.2 to −6.0 mV. An ionic strength of ~1 mM is too small for electrostatic stabilization, so CP likely stabilizes the droplets mainly through steric/electrostatic repulsion. The average particle size of the emulsions ranged from 8.98 ± 0.06 µm to 11.32 ± 0.03 µm. Formula 1 exhibited the smallest particle size (8.98 ± 0.06 µm), while Formula 4 exhibited the largest particle size (11.32 ± 0.03 µm). Smaller oil concentrations, in combination with a higher wall material

ratio (coffee pectin and maltodextrin), tended to produce smaller droplets due to the higher availability of emulsifiers around each droplet during homogenization. This finding is consistent with previous studies, which suggest that a lower oil-to-wall ratio results in smaller droplet sizes and better stability [23–27].

Table 2. Viscosity, electrical conductivity, zeta potential, and particle size properties of emulsion samples.

Formula	Viscosity (cP)	Electrical Conductivity (mS/cm)	Zeta Potential (mV)	Particle Size (μm)
1	12.50 ± 0.20 ^{c}	5.77 ± 0.04 ^{c}	−6.00 ± 0.07 ^{a}	8.98 ± 0.06 ^{c}
2	12.89 ± 0.17 ^{c}	5.88 ± 0.04 ^{c}	−6.15 ± 0.08 ^{a}	9.11 ± 0.06 ^{c}
3	13.20 ± 0.20 ^{b}	6.14 ± 0.02 ^{b}	−6.90 ± 0.10 ^{b}	10.22 ± 0.03 ^{b}
4	14.89 ± 0.01 ^{a}	6.51 ± 0.04 ^{a}	−7.17 ± 0.21 ^{c}	11.32 ± 0.03 ^{a}

One-way ANOVA was used to assess differences between formulas, followed by Tukey's HSD post hoc test. ± values are standard deviations between different replicates. Different letters indicate statistically significant differences between formulas at a significance level of $p < 0.05$.

3.1.2. Color and Light Microscopic Images

The color characteristics of the emulsions (Table 3) were influenced by the varying oil content, maltodextrin concentration, and core–wall ratio. The increasing lightness (L*) from Formula 1 to Formula 4 was consistent with increased oil content and droplet size, which can enhance light scattering and contribute to a lighter color [28]. The red-green axis (a*) and blue-yellow axis (b*) remained relatively low, suggesting that the emulsions maintained a neutral coloration with slight variations depending on the formulation's specific composition. The overall reduction in the intensity of color (both a* and b*) with increasing oil content could be due to the influence of oil on pigment distribution and the effect of droplet size on light reflection and scattering. The use of coffee pectin as a stabilizer may have also contributed to maintaining a stable color by preventing pigment migration, which is crucial for ensuring consistent product appearance [29].

Table 3. Color characteristics of emulsion samples.

Formula	L* (-)	a* (-)	b* (-)
1	18.31 ± 0.02 ^{d}	0.09 ± 0.006 ^{a}	−0.24 ± 0.01 ^{d}
2	20.57 ± 0.01 ^{c}	0.07 ± 0.002 ^{b}	−0.19 ± 0.00 ^{c}
3	28.04 ± 0.21 ^{b}	0.02 ± 0.010 ^{c}	−0.11 ± 0.02 ^{b}
4	32.16 ± 0.02 ^{a}	0.02 ± 0.010 ^{c}	−0.07 ± 0.02 ^{a}

One-way ANOVA was used to assess differences between formulas, followed by Tukey's HSD post hoc test. Different letters indicate statistically significant differences between formulas at a significance level of $p < 0.05$.

The microscopic images reveal differences in the droplet distribution, size, and density across the four emulsion formulations (Figure 1). In all four images, the emulsion droplets appear dispersed throughout the continuous phase. There was a noticeable increase in droplet size from the top left to the bottom right images, consistent with the trends observed in the particle size data presented in Table 2. The images also provide information about the uniformity of droplet size. Formula 1 shows relatively uniform droplets, although the droplet density appears to be higher due to a lower oil concentration (3%) and a higher ratio of wall materials.

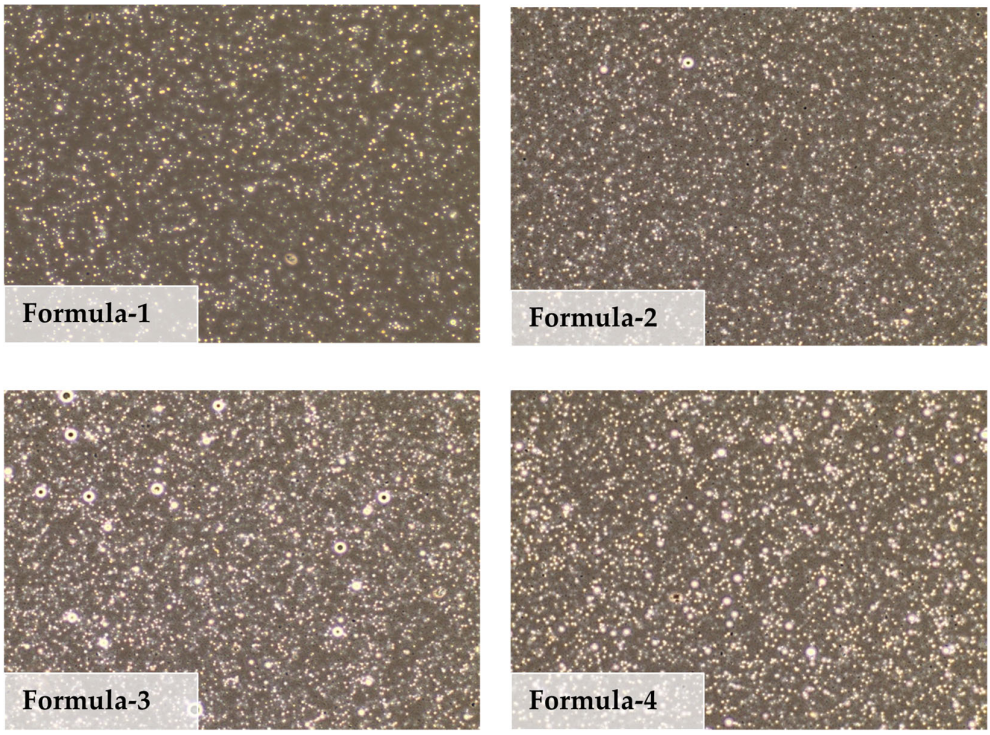

Figure 1. Light microscopic images (at 40× magnification) of emulsions (qualitative only).

3.2. Physicochemical Properties of Encapsulated Powders

3.2.1. Moisture Content, Water Activity, Particle Size, Wettability, Solubility, Bulk, and Tapped Densities

Table 4 presents the results of moisture content (MC), water activity (a_w), particle size, wettability, solubility, bulk density, and tapped density for the spray-dried encapsulated hemp oil samples. The MC of the encapsulated powders ranged from 2.75 ± 0.03% (Formula 4) to 2.97 ± 0.02% (Formula 1). Water activity (a_w) values varied slightly between 0.07 ± 0.001 and 0.08 ± 0.002, indicating that all formulations were well below the threshold for microbial activity. Similarly, Kelly et al. [30] also reported that encapsulated powders with an a_w below 0.2 are suitable for long-term storage due to reduced quality degradation. Botrel et al. [31] also emphasized that low moisture content minimizes oxidative degradation, which is essential for sensitive oils like hemp oil.

Table 4. Moisture content, water activity, particle size, wettability, solubility, bulk and tapped densities of spray-dried encapsulated samples.

	Formula 1	Formula 2	Formula 3	Formula 4
MC (%)	2.97 ± 0.02 ^{a}	2.81 ± 0.03 ^{c}	2.89 ± 0.02 ^{b}	2.75 ± 0.03 ^{c}
a_w	0.07 ± 0.001 ^{b}	0.08 ± 0.001 ^{a}	0.08 ± 0.002 ^{ab}	0.07 ± 0.002 ^{ab}
Particle size	5.00 ± 0.02 ^{c}	5.92 ± 0.13 ^{c}	7.65 ± 0.50 ^{b}	9.43 ± 0.01 ^{a}
Wettability (s)	355.7 ± 4.04 ^{d}	383.33 ± 0.6 ^{c}	401.7 ± 2.10 ^{b}	426.33 ± 0.60 ^{a}
Solubility (%)	89.57 ± 0.21 ^{a}	87.20 ± 0.26 ^{b}	88.67 ± 0.21 ^{c}	88.13 ± 0.15 ^{c}
Bulk density (g/mL)	0.21 ± 0.02 ^{c}	0.24 ± 0.02 ^{c}	0.29 ± 0.01 ^{b}	0.31 ± 0.02 ^{a}
Tapped density (g/mL)	0.43 ± 0.01 ^{c}	0.48 ± 0.02 ^{c}	0.59 ± 0.02 ^{b}	0.64 ± 0.04 ^{a}

One-way ANOVA was used to assess differences between formulas, followed by Tukey's HSD post hoc test. Different letters indicate statistically significant differences between formulas at a significance level of $p < 0.05$.

The particle size of encapsulated samples varied between 5.00 ± 0.02 µm and 9.43 ± 0.01 µm ($p < 0.05$), which is similar to results obtained by Madene et al. [32], where they noted that particle sizes in the range of 1–10 µm are typical for spray-dried emulsions. The smaller particle sizes observed in formulations with lower oil contents (Formulas 1 and 2) are consistent with the findings of Jafari et al. [33], who reported that higher emulsifier-to-oil ratios lead to better dispersion of oil droplets, resulting in smaller particles. Larger particle sizes observed in Formula 4 may be a consequence of increased oil content, leading to larger emulsion droplets during the drying process, similar to the findings of Tonon et al. [15] for flaxseed oil emulsions. The wettability times recorded ranged from 355.67 ± 4.04 to 426.33 ± 0.58 s ($p < 0.05$), with increased times observed for formulations with higher oil content (e.g., Formula 4). Wettability is influenced by particle size, surface hydrophilicity, and the nature of the wall material. Larger particle sizes, as well as increased oil loading, result in reduced surface area and decreased hydrophilicity, thus increasing wettability times. The findings are consistent with those reported by Ray et al. [34], who observed that high oil encapsulation typically results in hydrophobic surface characteristics, leading to increased wettability times. The high solubility observed across all formulations is similar to that reported by Desai and Park [35], who found that spray drying with wall materials such as maltodextrin results in high solubility due to its rapid dissolution in water. The significant difference between Formula 1 and the rest of the samples in terms of solubility may be linked to particle size and the ratio of core-to-wall material, consistent with observations by Jafari et al. [33], who found that smaller particle sizes result in increased solubility due to greater surface area for interaction with water.

Both the bulk and tapped densities of the encapsulated powders significantly increased from 0.21 ± 0.02 to 0.31 ± 0.02 g/mL and from 0.43 ± 0.01 to 0.64 ± 0.04 g/mL, respectively ($p < 0.05$). Higher bulk and tapped densities are indicative of better packing properties, which can be advantageous for transportation and storage [36]. Formulations with higher bulk/tapped density show tighter bed packing and less interparticle void space, which may limit oxygen access at the powder-bed scale, as suggested by Goula and Adamopoulos [37]. On the other hand, lower density values, such as those observed in Formulas 1 and 2, may be beneficial for applications where rapid dissolution is desired, such as in instant beverage formulations.

3.2.2. Particle Size Distributions and Morphology

The particle size distributions (Figure 2) for the four formulations exhibit distinct patterns, reflecting variations in droplet formation during emulsification and subsequent spray drying.

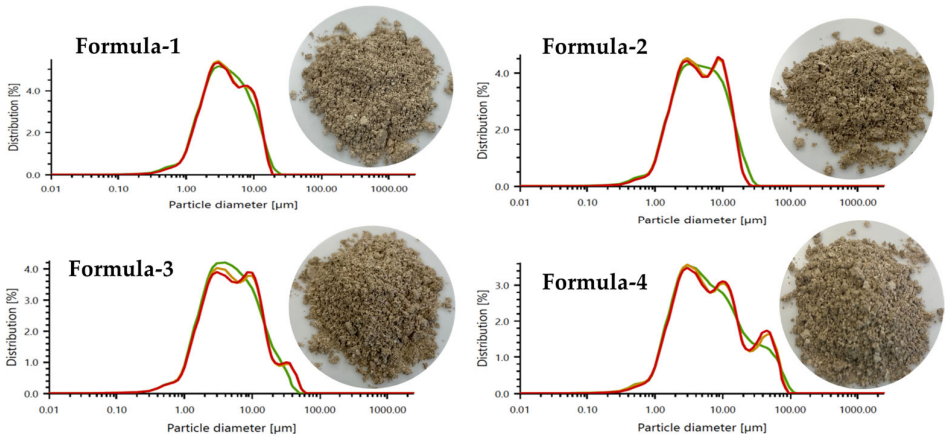

Figure 2. Particle size distributions (colored curves (red, green, orange) denote three independent replicates per formula) and images of encapsulated powders (qualitative only).

Each graph shows the presence of multiple peaks, indicating the particle size distribution of the samples. The main peaks for the formulations fall within the size range of approximately 1 to 100 μm. In particular, Formula 1 (top left) displays a narrower distribution compared to the others, with a pronounced peak at around 10 μm, suggesting a more homogeneous particle size. This narrower distribution aligns with the lower polydispersity index (PDI), and smaller average particle size observed in Table 1, indicating a well-dispersed emulsion with relatively uniform particles [24]. On the other hand, Formula 4 (bottom right) exhibits a broader distribution, with peaks extending into larger particle size ranges (over 100 μm). This broader distribution indicates greater polydispersity and less uniformity, which can be attributed to higher oil content and reduced emulsifier concentration in the formulation. The findings are consistent with the results of other studies, such as Madene et al. [32], which noted that higher oil concentrations tend to produce larger and less uniform particle sizes due to increased droplet coalescence.

The scanning electron micrographs (SEM) of the spray-dried microcapsules provide a detailed view of the surface morphology and structural characteristics of the encapsulated hemp oil particles (Figure 3). These micrographs are important for understanding the physical properties, encapsulation efficiency, and potential stability of the powders.

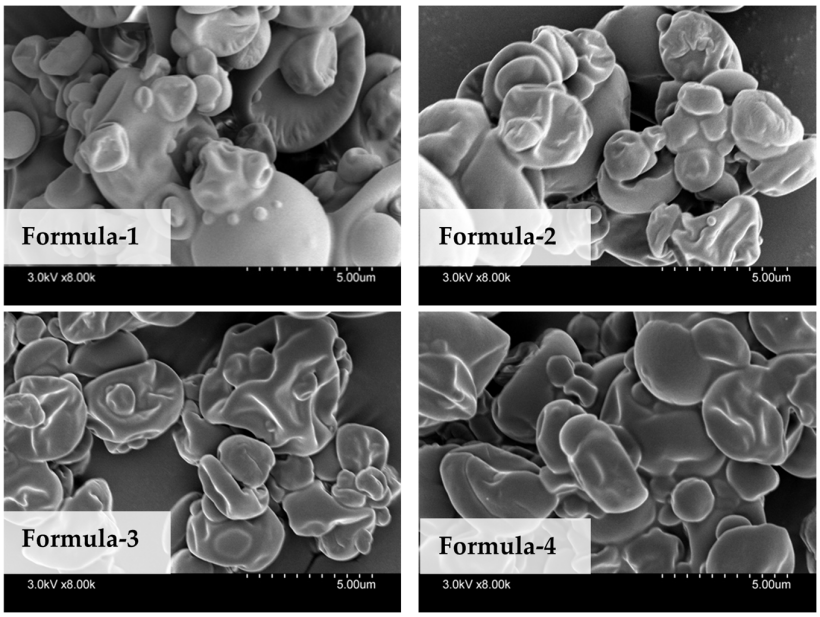

Figure 3. Scanning micrographs of spray-dried microcapsules.

All four images show spherical microcapsules with varying degrees of surface smoothness and shrinkage. The microcapsules in Formula 1 (top left) appear relatively smooth, with few visible dents or folds. This smooth surface is indicative of efficient encapsulation and proper spray drying conditions, which help prevent surface collapse during solvent evaporation [38]. In contrast, the microcapsules from Formula 4 (bottom right) exhibit rougher surfaces with more pronounced wrinkles and dents, indicating some degree of collapse or deformation during drying. This phenomenon is often attributed to higher oil content and reduced wall material availability, which can result in weaker film formation and structural instability. Such defects could compromise the protective barrier around the oil, potentially affecting its oxidative stability [15].

Overall, the differences observed in the powder morphology emphasize the importance of optimizing the core-to-wall ratio and spray drying conditions to achieve uniform and stable microcapsules. The use of an adequate amount of wall material is essential to

create a strong encapsulating film, reduce surface imperfections, and maintain the integrity of the microcapsules.

3.2.3. Encapsulation Efficiencies, Oil Release Characteristics, and Peroxide Values

Table 5 presents both the encapsulation efficiency (EE) and peroxide values (PV) for the spray-dried encapsulated hemp oil samples across four different formulations. Encapsulation efficiency is a measure of how effectively the core material, hemp oil, is entrapped within the wall matrix, while peroxide value serves as an indicator of the degree of lipid oxidation, reflecting the stability of the encapsulated oil [39].

Table 5. Encapsulation efficiencies (EE) and peroxide values (PV) of spray-dried encapsulated samples.

Formula	Encapsulation Efficiency (%)	Peroxide Value (meq O_2/kg Oil)
1	70.80 ± 0.25 ^{a}	10.70 ± 0.03 ^{d}
2	68.50 ± 0.12 ^{b}	11.00 ± 0.01 ^{c}
3	65.80 ± 0.70 ^{c}	11.23 ± 0.03 ^{b}
4	63.30 ± 0.12 ^{d}	11.40 ± 0.02 ^{a}

One-way ANOVA was used to assess differences between formulas, followed by Tukey's HSD post hoc test. Different letters indicate statistically significant differences between formulas at a significance level of $p < 0.05$.

The highest encapsulation efficiency was observed in Formula 1 (70.77 ± 0.25%), while the lowest was recorded for Formula 4 (63.27 ± 0.12%). The decrease in encapsulation efficiency with increasing oil content is consistent with previous findings in the literature. This trend can be attributed to the reduced availability of wall material, which limits the ability to form an effective encapsulating layer around each droplet. As the oil concentration increases, the emulsifier and wall material become less effective in covering the oil, resulting in decreased EE [40–42].

The PV for the four formulations ranged from 10.69 ± 0.03 meq O_2/kg oil in Formula 1 to 11.37 ± 0.02 meq O_2/kg oil in Formula 4. The significantly lower PV in Formula 1 compared to other samples ($p < 0.05$) suggests better oxidative stability, which correlates with the higher encapsulation efficiency. The lower PV in Formula 1 indicates that the wall materials provided an effective barrier against oxygen, thus limiting the oxidative degradation of the oil [38]. In contrast, Formula 4, which had the lowest encapsulation efficiency, also exhibited the highest peroxide value. This suggests that the lower EE contributed to increased exposure of the oil to oxygen, leading to higher lipid oxidation. This result is consistent with findings by Tonon et al. [15], who reported that reduced encapsulation efficiency and increased surface oil are associated with higher oxidation rates. The combination of EE and PV data provides valuable insights into the formulation and process parameters that influence the quality and stability of encapsulated oils. Future research could explore the use of alternative wall materials or co-encapsulants to further enhance encapsulation efficiency, particularly for high oil load formulations, and thereby improve oxidative stability.

Figure 4 presents the release profile of encapsulated hemp oil in simulated gastric fluid (SGF) and simulated intestinal fluid (SIF) for four different formulations. The release profiles in SGF and SIF provide insights into the stability and release behavior of the encapsulated oil under conditions that mimic the human digestive system. These data are critical for understanding the performance of the encapsulated formulations in terms of controlled release and bioavailability [43].

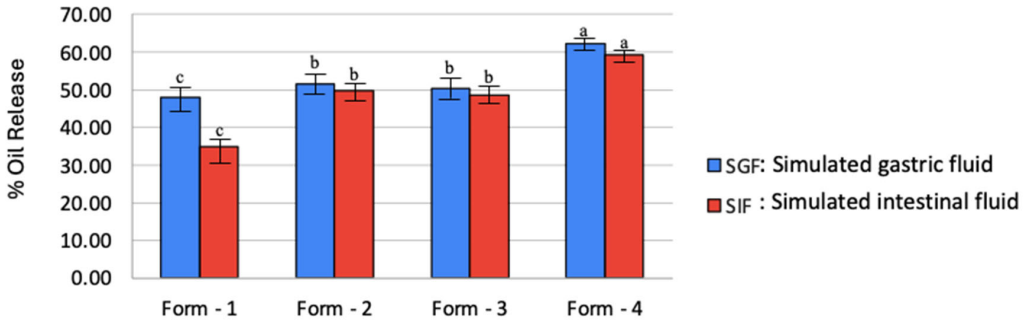

Figure 4. Release behavior of hemp oil microcapsules containing maltodextrin and coffee pectin in simulated gastric fluid (SGF) and simulated gastric and intestinal fluids (SIF). Different letters indicate statistically significant differences between formulas in terms of % oil release in SGF and SIF at a significance level of $p < 0.05$.

The release percentages in SGF are generally lower compared to those in SIF across all formulations. This trend indicates that the encapsulation effectively protects the hemp oil in the acidic environment of the stomach, delaying its release until it reaches the more neutral pH of the intestines. Under SGF (pH 1.2; pepsin), protonation of CP's carboxyl groups reduces its solubility and increases matrix cohesion, limiting oil diffusion and initial release. After transition to SIF (pH 6.8; pancreatin including lipase), deprotonation increases CP hydration while MD dissolves rapidly, opening diffusion pathways; concurrently, lipase activity at the oil–water interface accelerates release [44]. In SGF, Formula 1 exhibited the lowest release rate among the formulations ($p < 0.05$), indicating strong resistance to acidic conditions. The low release rate in SGF suggests that the combination of maltodextrin and coffee pectin provides a stable encapsulating matrix that can withstand the extreme gastric environment, effectively retaining the oil. Similar findings were reported by Madene et al. [32] and Rahmani et al. [45], where the use of polysaccharide-based wall materials resulted in delayed release in gastric conditions. Both Formulas 2 and 3 showed moderate release rates in SGF, indicating partial protection of the encapsulated oil. These formulations demonstrate significantly higher release percentages in SGF compared to Formula1 ($p < 0.05$), likely due to the increased oil content, which may have led to reduced encapsulation efficiency and slightly weakened the barrier effect. Formula 4 exhibited the highest release of SGF among all formulations ($p < 0.05$), indicating reduced stability in acidic conditions. This is consistent with the lower encapsulation efficiency observed for this formulation, as a less effective encapsulation leads to greater oil exposure and release in the gastric environment [46]. Formula 1 demonstrates a controlled release in SIF, suggesting gradual breakdown and enhanced bioavailability, which is ideal for targeted intestinal delivery. Formulas 2 and 3 show similar release profiles in SGF and SIF, indicating a balanced release mechanism responsive to pH changes. In contrast, Formula 4 exhibits the highest release rate in SIF among all other formulas ($p < 0.05$), likely due to its lower encapsulation efficiency and surface oil presence, which leads to faster breakdown and release in the intestinal environment. This trend highlights the influence of encapsulation efficiency on controlled release behavior in digestive conditions [47–49].

Overall, these findings support that encapsulation enables targeted release in the digestive tract and improves the stability and integrity of bioactive compounds.

4. Conclusions

This study highlights the potential of coffee pectin and maltodextrin as sustainable and functional wall materials for the microencapsulation of hemp seed oil using spray drying. The results confirm that the selection of encapsulating agents and process conditions significantly impacts the physicochemical properties, oxidative stability, apparent encapsu-

lation efficiency, and release kinetics of microcapsules. Notably, coffee pectin, derived from agricultural byproducts, not only enhances emulsion stability and encapsulation efficiency but also aligns with circular economy principles by valorizing food waste. Among the formulations tested, those with lower oil content (Formula 1) exhibited superior encapsulation efficiency, smaller particle size, and enhanced oxidative stability, while higher oil loadings (Formula 4) resulted in reduced encapsulation performance and increased lipid oxidation. The findings underscore the efficacy of coffee pectin and maltodextrin in creating stable microcapsules with controlled release profiles, which are crucial for applications in food and nutraceutical industries. Future research could explore the use of alternative wall material combinations, optimize encapsulation conditions, and investigate the bioavailability of encapsulated compounds to expand the utility of this approach. This study was limited by a lack of storage stability kinetics beyond time-zero PVs and no measurements of matrix Tg or moisture sorption/isotherms; these gaps will be addressed in future work.

Overall, this work contributes to the advancement of sustainable food processing technologies and the development of value-added products from underutilized biomass, supporting both environmental and industry objectives.

Author Contributions: Conceptualization, O.K. and G.E.P.; data curation, O.K. and G.E.P.; formal analysis, O.K. and G.E.P.; funding acquisition, C.F.; investigation, O.K. and G.E.P.; methodology, O.K. and G.E.P.; project administration, C.F.; resources, C.F.; software, O.K.; supervision, C.F.; validation, O.K., G.E.P., and C.F.; visualization, O.K.; writing—original draft, O.K. and G.E.P.; writing—review and editing, O.K., G.E.P. and C.F. All authors have read and agreed to the published version of the manuscript.

Funding: This research received no external funding.

Institutional Review Board Statement: Not applicable.

Informed Consent Statement: Not applicable.

Data Availability Statement: Despite all information has been provided herein, raw data are available upon request to the corresponding author.

Conflicts of Interest: Ozan Kahraman, Greg E. Petersen and Christine Fields are employees of Applied Food Sciences Inc. Applied Food Sciences provided the funding and materials for this study. The company's authors had no influence on the correctness and fairness of the research results.

Abbreviations

AOCS	American Oil Chemists' Society
ANOVA	Analysis of variance
a_w	Water activity
CI	Carr index
CP	Coffee pectin
DE	Dextrose equivalent
DI	Deionized (water)
D10, D50, D90	Particle diameters at 10%, 50%, and 90% of cumulative volume, respectively
DLS	Dynamic light scattering
EE	Encapsulation efficiency
ELS	Electrophoretic light scattering
HSD	Tukey's honestly significant difference (post hoc test)
L*, a*, b*	CIE color coordinates (lightness, green–red, blue–yellow)
MD	Maltodextrin
PDI	Polydispersity index
PV	Peroxide value
SEM	Scanning electron microscopy/microscope

SGF	Simulated gastric fluid
SIF	Simulated intestinal fluid
S.D.	Standard deviation
TD	Tapped density

References

1. Shen, P.; Gao, Z.; Fang, B.; Rao, J.; Chen, B. Ferreting out the secrets of industrial hemp protein as emerging functional food ingredients. *Trends Food Sci. Technol.* **2021**, *112*, 1–15. [CrossRef]
2. Kahraman, O.; Petersen, G.E.; Fields, C. Physicochemical and functional modifications of hemp protein concentrate by the application of ultrasonication and pH shifting treatments. *Foods* **2022**, *11*, 587. [CrossRef] [PubMed]
3. Karabulut, G.; Kahraman, O.; Pandalaneni, K.; Kapoor, R.; Feng, H. A comprehensive review on hempseed protein: Production, functional and nutritional properties, novel modification methods, applications, and limitations. *Int. J. Biol. Macromol.* **2023**, *253*, 127240. [CrossRef] [PubMed]
4. Speranza, B.; Petruzzi, L.; Bevilacqua, A.; Gallo, M.; Campaniello, D.; Sinigaglia, M.; Corbo, M.R. Encapsulation of active compounds in fruit and vegetable juice processing: Current state and perspectives. *J. Food Sci.* **2017**, *82*, 1291–1301. [CrossRef]
5. Naidu, H.; Kahraman, O.; Feng, H. Novel applications of ultrasonic atomization in the manufacturing of fine chemicals, pharmaceuticals, and medical devices. *Ultrason. Sonochem.* **2022**, *86*, 105984. [CrossRef]
6. Jafari, S.; Jafari, S.M.; Ebrahimi, M.K.; Kijpatanasilp, I.; Assatarakul, K. A decade overview and prospect of spray drying encapsulation of bioactives from fruit products: Characterization, food application and in vitro gastrointestinal digestion. *Food Hydrocoll.* **2023**, *134*, 108062. [CrossRef]
7. Akbarbaglu, Z.; Peighambardoust, S.H.; Sarabandi, K.; Jafari, S.M. Spray drying encapsulation of bioactive compounds within protein-based carriers; different options and applications. *Food Chem.* **2021**, *359*, 129965. [CrossRef]
8. Karrar, E.; Mahdi, A.A.; Steth, S.; Ahmed, I.A.M.; Manzoor, M.F.; Wei, W.; Wang, X. Effects of maltodextrin combination with gum Arabic and whey protein isolate on the microencapsulation of gurum seed oil using a spray drying method. *Int. J. Biol. Macromol.* **2021**, *171*, 208–216. [CrossRef]
9. Reichembach, L.H.R.; Petkowicz, C.L.O. Extraction and characterization of a pectin from coffee (*Coffea arabica* L.) pulp with gelling properties. *Carbohydr. Polym.* **2020**, *245*, 116473. [CrossRef]
10. Chamyuang, S.; Duangphet, S.; Owatworakit, A.; Intatha, U.; Nacha, J.; Kerdthong, P. Preparation of pectin films from coffee cherry and its antibacterial activity. *Trends Sci.* **2021**, *18*, 34. [CrossRef]
11. Biratu, G.; Gonfa, G.; Bekele, M.; Woldemariam, H.W. Extraction and characterization of pectin from coffee (*Coffea arabica* L.) pulp obtained from four different coffee producing regions. *Int. J. Biol. Macromol.* **2024**, *274*, 133321. [CrossRef]
12. Laureanti, E.J.G.; Paiva, T.S.; Jorge, L.M.M.; Jorge, R.M.M. Microencapsulation of bioactive compound extracts using maltodextrin and gum arabic by spray and freeze-drying techniques. *Int. J. Biol. Macromol.* **2023**, *253*, 126969. [CrossRef]
13. Misono, T.; Dynamic Light Scattering (DLS); Abe, M. (Eds.) *Measurement Techniques and Practices of Colloid and Interface Phenomena*; Springer: Singapore, 2019; pp. 65–69. [CrossRef]
14. Lekjing, S.; Keawpeng, I.; Venkatachalam, K.; Karrila, S. Impact of different sugar types and their concentrations on salted duck egg white based meringues. *Foods* **2022**, *11*, 1248. [CrossRef] [PubMed]
15. Tonon, R.V.; Grosso, C.R.; Hubinger, M.D. Influence of emulsion composition and inlet air temperature on the microencapsulation of flaxseed oil by spray drying. *Food Res. Int.* **2011**, *44*, 282–289. [CrossRef]
16. Fuchs, M.; Turchiuli, C.; Bohin, M.; Cuvelier, M.E.; Ordonnaud, C.; Maillard, M.N.; Dumoulin, E. Encapsulation of oil in powder using spray drying and fluidized bed agglomeration. *J. Food Eng.* **2006**, *75*, 27–35. [CrossRef]
17. Karaca, A.C.; Low, N.; Nickerson, M. Encapsulation of flaxseed oil using a benchtop spray dryer for legume protein-maltodextrin microcapsule preparation. *J. Agric. Food Chem.* **2013**, *61*, 5148–5155. [CrossRef]
18. AOCS. AOCS Official method Cd 8-53. In *Official Methods and Recommended Practices of the American Oil Chemists' Society Method Cd 8-53. Peroxide Value Acetic Acid–Chloroform Method*, 4th ed.; Gunstone, F., Ed.; AOCS Press: Champaign, IL, USA, 1993.
19. Saifullah, M.; Yusof, Y.A.; Aziz, M.G. Physicochemical and flow properties of fruit powder and their effect on the dissolution of fast dissolving fruit powder tablets. *Powder Technol.* **2016**, *301*, 396–404. [CrossRef]
20. Fernandes, R.V.D.B.; Borges, S.V.; Silva, E.K.; Da Silva, Y.F.; De Souza, H.J.B.; Do Carmo, E.L.; De Oliveira, C.R.; Yoshida, M.I.; Botrel, D.A. Study of ultrasound-assisted emulsions on microencapsulation of ginger essential oil by spray drying. *Ind. Crops Prod.* **2016**, *94*, 413–423. [CrossRef]
21. Battista, C.A.; Constenla, D.; Ramírez-Rigo, M.V.; Piña, J. The use of arabic gum, maltodextrin, and surfactants in the microencapsulation of phytosterols by spray drying. *Powder Technol.* **2015**, *286*, 193–201. [CrossRef]
22. Mahalakshmi, L.; Choudhary, P.; Moses, J.; Anandharamakrishnan, C. Emulsion electrospraying and spray drying of whey protein nano and microparticles with curcumin. *Food Hydrocoll. Health* **2023**, *3*, 100122. [CrossRef]

23. Noello, C.; Carvalho, A.; Silva, V.; Hubinger, M. Spray dried microparticles of chia oil using emulsion stabilized by whey protein concentrate and pectin by electrostatic deposition. *Food Res. Int.* **2016**, *89*, 549–557. [CrossRef]
24. Jafari, S.M.; Assadpoor, E.; He, Y.; Bhandari, B. Encapsulation Efficiency of Food Flavours and Oils during Spray Drying. *Dry. Technol.* **2008**, *26*, 816–835. [CrossRef]
25. Sanchez, M.D.R.H.; Cuvelier, M.; Turchiuli, C. Design of liquid emulsions to structure spray dried particles. *J. Food Eng.* **2015**, *167*, 99–105. [CrossRef]
26. Taboada, M.L.; Heiden-Hecht, T.; Brückner-Gühmann, M.; Karbstein, H.P.; Drusch, S.; Gaukel, V. Spray drying of emulsions: Influence of the emulsifier system on changes in oil droplet size during the drying step. *J. Food Process. Preserv.* **2021**, *45*, e15753. [CrossRef]
27. Wang, X.; Ding, Z.; Zhao, Y.; Prakash, S.; Liu, W.; Han, J.; Wang, Z. Effects of lutein particle size in embedding emulsions on encapsulation efficiency, storage stability, and dissolution rate of microencapsules through spray drying. *LWT* **2021**, *146*, 111430. [CrossRef]
28. Giorgio, L.; Salgado, P.R.; Mauri, A.N. Encapsulation of fish oil in soybean protein particles by emulsification and spray drying. *Food Hydrocoll.* **2019**, *87*, 891–901. [CrossRef]
29. Lima, P.M.; Dacanal, G.C.; Pinho, L.S.; Pérez-Córdoba, L.J.; Thomazini, M.; Moraes, I.C.F.; Favaro-Trindade, C.S. Production of a rich-carotenoid colorant from pumpkin peels using oil-in-water emulsion followed by spray drying. *Food Res. Int.* **2021**, *148*, 110627. [CrossRef] [PubMed]
30. Kelly, G.M.; O'Mahony, J.A.; Kelly, A.L.; O'Callaghan, D.J. Physical characteristics of spray-dried dairy powders containing different vegetable oils. *J. Food Eng.* **2014**, *122*, 122–129. [CrossRef]
31. Botrel, D.A.; Borges, S.V.; Fernandes, B.; Viana, A.D.; Marques, G.R. Evaluation of spray drying conditions on properties of microencapsulated oregano essential oil. *Int. J. Food Sci. Technol.* **2012**, *47*, 2289–2296. [CrossRef]
32. Madene, A.; Jacquot, M.; Scher, J.; Desobry, S. Flavour encapsulation and controlled release—A review. *Int. J. Food Sci. Technol.* **2006**, *41*, 1–21. [CrossRef]
33. Jafari, S.M.; He, Y.; Bhandari, B. Role of Powder Particle Size on the Encapsulation Efficiency of Oils during Spray Drying. *Dry. Technol.* **2007**, *25*, 1081–1089. [CrossRef]
34. Ray, S.; Raychaudhuri, U.; Chakraborty, R. An overview of encapsulation of active compounds used in food products by drying technology. *Food Biosci.* **2016**, *13*, 76–83. [CrossRef]
35. Desai, K.G.H.; Park, H.J. Encapsulation of vitamin C in tripolyphosphate cross-linked chitosan microspheres by spray drying. *J. Microencapsul.* **2005**, *22*, 179–192. [CrossRef] [PubMed]
36. Rosenberg, M.; Sheu, T. Microencapsulation of volatiles by spray-drying in whey protein-based wall systems. *Int. Dairy J.* **1996**, *6*, 273–284. [CrossRef]
37. Goula, A.M.; Adamopoulos, K.G. Effect of Maltodextrin Addition during Spray Drying of Tomato Pulp in Dehumidified Air: II. Powder Properties. *Dry. Technol.* **2008**, *26*, 726–737. [CrossRef]
38. Gharsallaoui, A.; Roudaut, G.; Chambin, O.; Voilley, A.; Saurel, R. Applications of spray-drying in microencapsulation of food ingredients: An overview. *Food Res. Int.* **2007**, *40*, 1107–1121. [CrossRef]
39. Roccia, P.; Martínez, M.L.; Llabot, J.M.; Ribotta, P.D. Influence of spray-drying operating conditions on sunflower oil powder qualities. *Powder Technol.* **2014**, *254*, 307–313. [CrossRef]
40. Turasan, H.; Sahin, S.; Sumnu, G. Encapsulation of rosemary essential oil. *LWT Food Sci. Technol.* **2015**, *64*, 112–119. [CrossRef]
41. Ozdemir, N.; Bayrak, A.; Tat, T.; Altay, F.; Kiralan, M.; Kurt, A. Microencapsulation of basil essential oil: Utilization of gum arabic/whey protein isolate/maltodextrin combinations for encapsulation efficiency and in vitro release. *J. Food Meas. Charact.* **2021**, *15*, 1865–1876. [CrossRef]
42. Selim, K.A.; Alharthi, S.S.; Abu El-Hassan, A.M.; Elneairy, N.A.; Rabee, L.A.; Abdel-Razek, A.G. The Effect of Wall Material Type on the Encapsulation Efficiency and Oxidative Stability of Fish Oils. *Molecules* **2021**, *26*, 6109. [CrossRef]
43. Grifoni, L.; Vanti, G.; Bilia, A.R. Nanostructured Lipid Carriers Loaded with Cannabidiol Enhance Its Bioaccessibility to the Small Intestine. *Nutraceuticals* **2023**, *3*, 210–221. [CrossRef]
44. Jia, C.; Huang, S.; Liu, R.; You, J.; Xiong, S.; Zhang, B.; Rong, J. Storage stability and in-vitro release behavior of microcapsules incorporating fish oil by spray drying. *Colloids Surf. A Physicochem. Eng. Asp.* **2021**, *628*, 127234. [CrossRef]
45. Rahmani-Manglano, N.E.; Tirado-Delgado, M.; García-Moreno, P.J.; Guadix, A.; Guadix, E.M. Influence of emulsifier type and encapsulating agent on the in vitro digestion of fish oil-loaded microcapsules produced by spray-drying. *Food Chem.* **2022**, *392*, 133257. [CrossRef]
46. Kosaraju, S.L.; Weerakkody, R.; Augustin, M.A. In-vitro evaluation of hydrocolloid–based encapsulated fish oil. *Food Hydrocoll.* **2009**, *23*, 1413–1419. [CrossRef]
47. Lim, W.; Nyam, K. Characteristics and controlled release behaviour of microencapsulated kenaf seed oil during in-vitro digestion. *J. Food Eng.* **2016**, *182*, 26–32. [CrossRef]

48. Azad, A.K.; Abdullah, S.M.; Chatterjee, B.; Wan Sulaiman, W.M.; Elsayed, T.M.; Doolaanea, A.A. Encapsulation of Black Seed Oil in Alginate Beads as a pH-Sensitive Carrier for Intestine-Targeted Drug Delivery: In Vitro, In Vivo and Ex Vivo Study. *Pharmaceutics* **2020**, *12*, 219. [CrossRef] [PubMed]
49. Bai, G.; Zhao, M.; Chen, W.; Ma, G.; Ma, Y.; Xianqing, H. Fabrication, characterization and simulated gastrointestinal digestion of sea buckthorn pulp oil microcapsule: Effect of wall material and interfacial bilayer stabilization. *J. Sci. Food Agric.* **2025**, *105*, 1737–1744. [CrossRef] [PubMed]